ACS APPLIED MATERIALS & INTERFACES

Research Article

www.acsami.org

Programming of Shape Memory Natural Rubber for Near-Discrete Shape Transitions

Dominik Quitmann, Frauke M. Reinders, Benjamin Heuwers, Frank Katzenberg, and Joerg C. Tiller*

Chair of Biomaterials & Polymer Science, Department of Biochemical & Chemical Engineering, TU Dortmund, D-44221 Dortmund, Germany

Supporting Information

ABSTRACT: Typical shape memory polymers are hot-programmed and show a shape transition over a broad temperature range of 10 K and more. Cold-programmed shape memory natural rubber (SMNR) recovers more than 80% of its original shape within 1 K. The trigger point can be increased upon aging the stretched SMNR over several weeks without losing the narrow trigger range. This process can be accelerated by treatment of the stretched SMNR with nonaffine solvent vapors. Affine solvent vapors of low concentrations afford higher trigger points than that achieved by aging. This way, even higher cross-linked natural rubber can be cold-programmed.

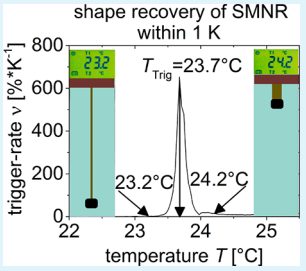

KEYWORDS: *narrow shape-transition, SMNR, shape memory, cold-programming, aging*

INTRODUCTION

Shape memory materials are capable of memorizing a temporary shape unless they are exposed to an external stimulus that triggers them to recover their permanent shape.[1] Although stimuli such as chemical vapors[2,3] or liquids,[4−7] mechanical stress,[8,9] IR/UV light,[10] or alternating magnetic fields[11] have been described, the majority of all shape memory materials is triggered thermally by heating above a certain material-dependent temperature, which is referred to as trigger temperature T_{trig}.[12] Generally, shape memory polymers (SMPs) do not recover their shape in full at this temperature but over a fairly broad range of several kelvin. For SMPs based on glassy polymers the trigger range is caused by the naturally broad glass transition. SMPs composed of semicrystalline polymers are triggered at the melting point, T_m, of the crystals, which usually stretches over a broad temperature range.[13,14] This is due to the dependence of T_m on crystal size and the naturally broad size distribution of those crystals. The same is true for liquid crystalline shape memory polymers.[15,16] Even shape memory alloys are often described to have a fairly broad trigger range.[17] Such behavior is sufficient for most applications of shape memory materials. However, there are several applications of smart materials that benefit from a discrete transition point such as safety systems, for example, valves, switches, and shape-adaptive medical devices.[18,19]

In contrast to most other SMPs, the recently discovered shape memory natural rubber (SMNR) fully recovers within 1 K when being cold-programmed.[20] The highest achievable trigger temperature upon cold-programming with the highest possible straining rate and the lowest possible degree of cross-linking (X_C) was found to be 26 °C, which is too low for most applications.

One common way to increase the trigger temperature is to program at higher temperatures.[21−24] A more recently discovered way of obtaining higher trigger temperatures of already programmed SMNRs is recrystallization of the constrained sample upon solvent vapor exposure.[25] Both methods allow increasing the trigger temperature of SMNR to up to 42 °C, but this comes at the expense of the exceptionally narrow trigger range of cold-programmed SMNR.

A possible explanation for the discrepancy between the trigger range of the cold-programmed SMNR, as well as the hot- and solvent-programmed SMNR, is that, in the first case, all crystals start growing simultaneously with the same rate. In the latter two scenarios, only a fraction of the crystals grow at the programming temperature or in the swollen network. After cooling or drying, more crystals of different size are formed, which broadens the melting range and thus the trigger range.

In the cause of investigations on SMNR, we observed that programmed samples show a higher T_{Trig} after several days of storage. To explore this in detail, we stretched SMNR with a X_C = 0.2% to 800% under ambient conditions and held in this state for up to 49 days. In intervals, samples were explored regarding their trigger behavior.[25] As shown in Figure 1, aging of the samples results in a significant increase in trigger temperature without losing the exceptionally narrow trigger range for up to 12 days. After this, the change of trigger temperature is negligible but the trigger range significantly broadens.

Additionally, higher cross-linked not cold-programmable NR with a X_C = 0.42% was stretched to 560% and clamped at ambient conditions for 4 days. After 1 h, the stress of the sample was released, and the NR completely recovered its original shape. In contrast, unclamping the sample after 4 days

Received: September 15, 2014
Accepted: December 23, 2014
Published: December 23, 2014

DOI: 10.1021/am507184c
ACS Appl. Mater. Interfaces 2015, 7, 1486−1490

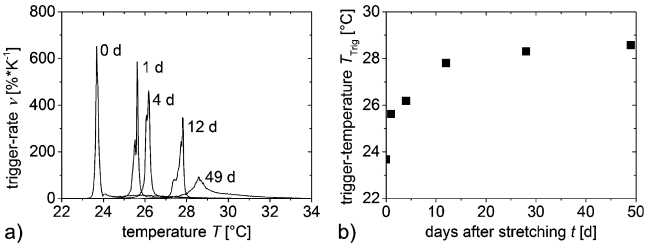

Figure 1. (a) Trigger processes of a SMNR samples (X_C = 0.2%, ε = 800%) directly after stretching and after 1, 4, 12, and 49 days of aging. (b) Depiction of the dependency of the trigger temperature on the days of aging after stretching.

resulted in a fixity of 70%, that is, the nonprogrammable NR was cold-programmed upon aging the stretched network.

To figure out if the effect is truly a shifting of the trigger point, we repeated the same experiment, and the samples were both cooled with liquid nitrogen prior to unclamping. Then, the samples were continuously heated in a TMA measuring the trigger temperature by monitoring the thickness increase. As shown in Figure 2, the aging process indeed causes a trigger temperature shift for 4 K (Table 1).

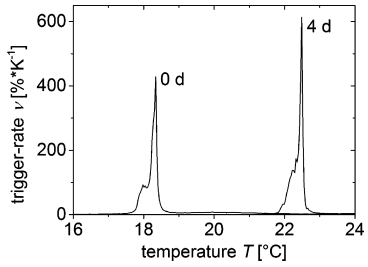

Figure 2. Trigger processes of stretched NR samples (X_C = 0.42%, ε = 560%), directly after stretching and after 4 days of aging, respectively.

Table 1. Trigger Temperatures and Fixity Ratios R_f of SMNR (X_C = 0.20) after 0, 1, 4, 12, and 49 Days of Aging and Natural Rubber (X_C = 0.42) after 0 and 4 Days of Aging

days of aging	$T_{Trig}(X_C = 0.20)$/ $T_{Trig}(X_C = 0.42)$ (°C)	$R_f(X_C = 0.20)/R_f(X_C = 0.42)$
0	23.7/18.3	0.69/0.69
1	25.6/–	0.62/–
4	26.2/22.5	0.67/0.71
12	27.8/–	0.53/–
49	28.6/–	0.55/–

A possible explanation for this behavior is the literature known lamellar thickening[26,27] which increases the melting point of crystals with time. In order to explore if this is the case for our samples aswell we monitored the width of the (002) reflection of stretched SMNR with time using wide-angle X-ray scattering (WAXS) experiments (Figure 3). According to these preliminary experiments no significant lamellar thickening but a slight increase in crystallinity was observed.

Although lamellar thickening does not seem to be the reason, the aging method is suited to increase the trigger temperature of stretched SMNR without broadening the trigger range. However, a time scale of weeks of programming of shape memory polymers is not practical. Thus, we investigated the possibility to accelerate the aging process by treatment with solvent vapor. We performed an initial experiment by treating a

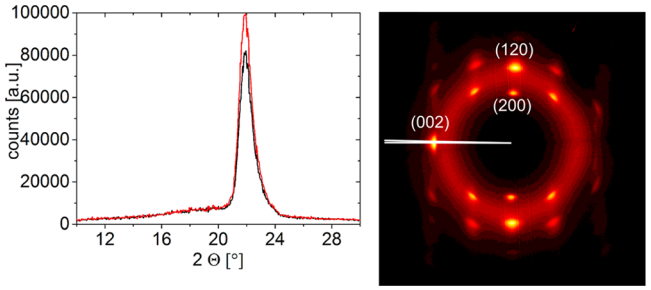

Figure 3. WAXS measuring of the (002) reflection (carried out with Bruker Nanostar) of stretched SMNR (X_C = 0.2, ε = 800%) using a bin-normalized integration ($\Delta\chi$ = 1°, 0° < 2θ < 30°). The sample was tilted by an angle of 10° to obtain the (002) reflection.

stretched SMNR (X_C = 0.2%, ε = 800%) with toluene vapor at equilibrium vapor pressure (EVP). This results in an inacceptable trigger width of about 30 K after 12 h of treatment, as shown in Figure 4.

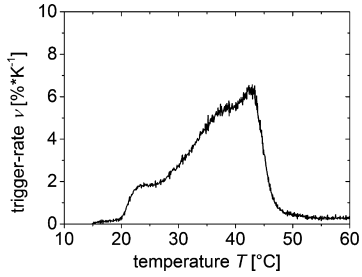

Figure 4. First derivative of the thickness increase versus temperature of a SMNR (X_C = 0.2, ε = 800%) after 12 h of treatment with toluene vapor at EVP and further 12 h of drying monitored with a thermal mechanical analyzer (TMA 2940, TA Instruments, Inc.).

A similar result was found in previous work where the same solvent was used to reprogram a stress-free constrained programmed SMNR.[25] We propose that good solvents at high concentrations swell the matrix of the polymer network to such an extent ($S_{toluene}$ = 4.67, X_C = 0.2%, ε = 800%) that already formed crystals collapse, and recrystallization occurs upon drying. This did not lead to narrow trigger ranges. To avoid high swelling, we used affine solvents at lower concentrations in the following.

Figure 5 shows the degrees of swelling S of stretched natural rubbers at different solvent concentrations. Values of the solvent vapor concentrations are listed in Table 2. The concentrations for the solvents were chosen to match the activities of 0.5, 0.7, and 0.9, respectively, of the EVP of each used solvent. It is clearly seen that decreasing the solvent vapor concentration drastically lowers S. This is a typical behavior of swelling of natural rubber.[28,29]

For example, toluene swells a stretched sample (X_C = 0.2%, ε = 800%) at EVP to S = 4.67. Lowering the solvent vapor concentration to 90% of this value (0.10 g L^{-1}) results in S = 1.36. The sample with X_C = 0.42 (ε = 560%) swells to S = 4.19 at EVP(toluene) and to S = 1.39 at 90% of EVP(toluene). Surprisingly, solvent vapor at concentrations below the respective equilibrium vapor pressure afford similar degrees of swelling for the two differently cross-linked stretched networks (Figure 5). Also, strain changes do not significantly affect the degree of swelling of those samples. For example, a sample with X_C = 0.2, stretched to 800%, shows only a slight decrease of

DOI: 10.1021/am507184c
ACS Appl. Mater. Interfaces 2015, 7, 1486−1490

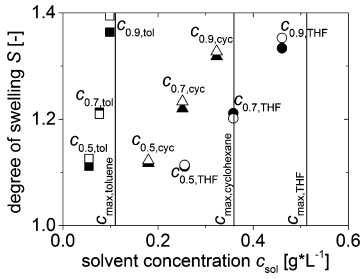

Figure 5. Dependency of the degree of swelling S on solvent vapor concentration after 12 h exposure to (▲ and Δ) cyclohexane, (■ and □) toluene, and (● and ○) THF. Experiments were performed with stretched SMNR (X_C = 0.2%, ε = 800%, solid symbols) and NR (X_C = 0.42%, ε = 560%, open symbols). The concentrations at EVP for the respective solvents are indicated by vertical lines.

Table 2. Applied Vapor Concentrations of Toluene, THF, and Cyclohexane and the Resulting Degrees of Swelling (S) of the Stretched Samples After 12 h of Exposure

label of concn	solvent vapor	concn (g L^{-1})	$S(X_C = 0.20)/S(X_C = 0.42)$
$C_{0.5,tol}$	toluene	0.06	1.11/1.12
$C_{0.7,tol}$	toluene	0.08	1.21/1.21
$C_{0.9,tol}$	toluene	0.10	1.36/1.39
$C_{0.5,THF}$	THF	0.26	1.11/1.11
$C_{0.7,THF}$	THF	0.36	1.21/1.20
$C_{0.9,THF}$	THF	0.46	1.33/1.35
$C_{0.5,cyc}$	cyclohexane	0.18	1.12/1.12
$C_{0.7,cyc}$	cyclohexane	0.25	1.22/1.23
$C_{0.9,cyc}$	cyclohexane	0.32	1.32/1.33

swelling from S = 1.51 to S = 1.36 compared to the unstretched sample. The same is true for the other affine solvents cyclohexane and THF. The lower solvent vapor concentrations were applied to the stretched cross-linked natural rubbers for 12 h, followed by 12 h of air drying, and subsequently, the trigger behavior was measured. Figure 6a,b depicts the trigger behavior of toluene vapor treated samples. Treating the SMNR sample with air containing 0.06 g L^{-1} toluene results indeed in a trigger shift of 6.5 K within 1d without losing the discrete trigger behavior. Increasing the toluene concentrations to 0.08 and 0.10 g L^{-1} results in greater shifts of 8.0 and 9.2 K, respectively. The NR sample shows similar shifts. Higher concentrations of toluene in the gas phase seem to broaden the trigger range slightly, but even at the highest applied concentration, 80% of the trigger process takes place within 1 K. Interestingly, toluene vapor treatment results in higher trigger points than pure aging alone even after 49 days. Treatment with THF also results in significant trigger point shifts without changing the narrow trigger range. The trigger shift cannot be strongly increased by raising the THF concentration above 0.26 g L^{-1}. Using cyclohexane vapor for trigger point shifting results in a high shift of 8.9 K. Varying the concentration of this compound does not affect the trigger shift but results in a slight broadening of the trigger range. In all cases, the affine solvents accelerate the aging process for obtaining higher trigger points with narrow trigger ranges. The shifts depend on the concentration and result in higher trigger points than aging alone.

Additionally, we explored if nonaffine solvents can be used for this purpose. Figure 7 shows the trigger behavior of

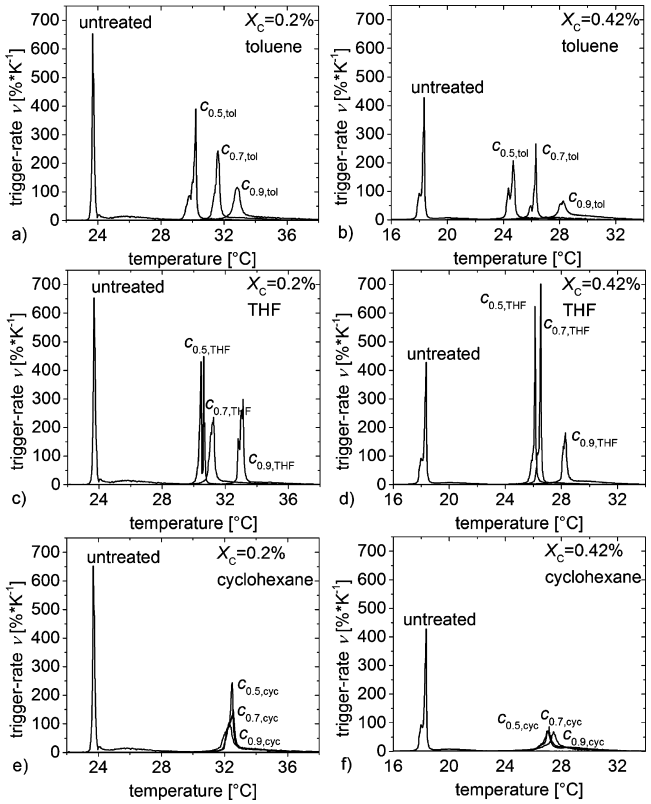

Figure 6. Trigger processes of stretched (a, c, and e) SMNR (X_C = 0.2%, ε = 800%) and (b, d, and f) NR (X_C = 0.42%, ε = 560%) before and after treatment with vapors of (a and b) toluene, (c and d) THF, and (e and f) cyclohexane. Solvent exposure time was 12 h at room temperature followed by air drying for 12 h. The respective solvent vapor concentrations are listed in Table 2.

stretched SMNR and cross-linked NR left over liquid acetone and ethanol for 12 h and subsequent drying for a further 12 h.

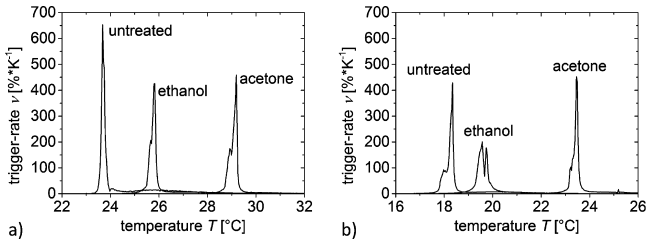

Figure 7. Trigger processes of stretched (a) SMNR (X_C = 0.2%, ε = 800%) and (b) NR (X_C = 0.42%, ε = 560%) directly after stretching and after treatment with vapors of ethanol and acetone, respectively, at EVP. Solvent exposure time was 12 h at room temperature followed by air drying for 12 h.

While ethanol treatment results in the same shift that was found after 1 day of aging, the acetone treated sample shows a shift of 5.5 K. This indicates that even nonaffine solvent vapors are capable of accelerating the trigger point shifting. In contrast to the affine solvent vapors, the highest achieved trigger point shift does not exceed that found for aging (Table 3).

Mechanistic Considerations. Because the aging effect and its acceleration by solvent vapor treatment does not correlate to changes of the crystal dimensions as approved by WAXS measurements we propose that the controlling parameter might be alteration of the microstructure of the noncrystalline phase.

DOI: 10.1021/am507184c
ACS Appl. Mater. Interfaces 2015, 7, 1486−1490

Table 3. Trigger Temperatures and Fixity Ratios, R_f, of SMNR (X_C = 0.2) and NR (X_C = 0.42) after Solvent Vapor Exposure[a]

label of concn	$T_{Trig}(X_C = 0.2)/T_{Trig}(X_C = 0.42)$ (°C)	$R_f(X_C = 0.2)/R_f(X_C = 0.42)$
$C_{0.5,tol}$	30.2/24.7	0.59/0.68
$C_{0.7,tol}$	31.6/26.3	0.58/0.59
$C_{0.9,tol}$	32.8/28.3	0.58/0.67
$C_{0.5,THF}$	30.6/26.1	0.55/0.71
$C_{0.7,THF}$	31.3/26.5	0.56/0.76
$C_{0.9,THF}$	33.1/28.3	0.59/0.69
$C_{0.5,cyc}$	32.5/27.0	0.55/0.47
$C_{0.7,cyc}$	32.3/27.1	0.53/0.59
$C_{0.9,cyc}$	32.5/27.4	0.56/0.59
toluene at EVP	42.9/–	0.48/–
ethanol at EVP	25.8/19.6	0.61/0.66
acetone at EVP	29.2/23.5	0.61/0.71

[a]Respective concentrations given in Table 2; air drying for 12 h.

This is supported by previously published findings where trigger points can be shifted by stressing the amorphous phase externally.[8,9] Taking this into account, the aging effect might be a slow reorganization of the stressed entanglements in the amorphous phase which were originally tensioned by straining the sample. This is supported by the literature known slow relaxation processes of strained natural rubber.[30,31] The influence of solvent vapors might be either acceleration of this relaxation (nonaffine solvent vapors) or a rearrangement of the microstructure (affine solvent vapors). To find whether the investigated SMNR is chemically altered during the storage, we determined M_C of the SMNR after 1 and 49 days of storage, respectively. Additionally, the 1 day old and the long-term stored sample were programmed and T_{Trig} was determined directly. The results are shown in the Supporting Information, Figures S1 and S2. M_C and T_{Trig} are the same for both samples, indicating that the SMNR is not chemically altered during storage.

CONCLUSION

Cold-programmed shape memory natural rubber exhibits one of the most narrow temperature-induced shape transitions of all shape memory materials. It was shown that the relatively low trigger temperature is increased by aging of the stretched sample without losing the narrow transition range. This way, even nonprogrammable higher cross-linked natural rubber can be cold-programmed. The process was significantly accelerated by exposing the stretched natural rubber samples to solvent vapors. While nonaffine solvents shift the trigger point faster but not further than aging does, affine solvents shift the trigger point to higher temperatures. Investigations of this process with WAXS measurements could not confirm the originally suggested lamellar thickening as reason for the higher trigger point. Further investigations will be necessary to fully understand this.

EXPERIMENTAL SECTION

Synthesis. Natural rubber (Standard Malaysian Rubber–SMR10) with an initial molecular weight of about 3 000 000 g mol^{-1} was masticated for 10 min using a heatable double-roller operated at 80 °C, subsequently mixed with dicumylperoxide (DCP) for 5 min and cross-linked in a heating press at 160 °C for 35 min. Using 0.2 and 0.5 parts per hundred rubber DCP resulted in an M_c of 34 000 g mol^{-1} (0.20% degree of cross-linking) and 16 000 g mol^{-1} (0.42% degree of crosslinking) measured according to the Mooney–Rivlin theory.[32] The samples are always stored in a desiccator in the dark.

SMNR Stretching and Solvent Treatment. SMNRs were stretched at room temperature (25 °C) to a strain of 560 and 800%, which is 80% of maximum strain (maximum strain is the fracture strain determined as average value of 10 samples), according to the degree of cross-linking, using a strain rate of 200% s^{-1}. Subsequently, the specimen was clamped in a holder to fix the strain. To treat the SMNR samples under constrained condition at the respective strain with different solvent vapor concentrations, we put the clamped sample into a closed chamber with the required solvent. The quantity of solvent was calculated according to the ideal gas law ($p_{sol} = n_{sol}RTV_{chamber}^{-1}$ with $n_{sol} = V_{sol}\rho M_{sol}^{-1}$). After solvent vapor treatment for 12 h, the sample was weighed using an analytical balance (Mettler Toledo XS105; accuracy, 10^{-4} g) to determine the degree of swelling. Subsequently, the samples were dried at room temperature (25 °C) for 12 h and then unclamped to measure their trigger behavior. All used solvents were of analytical grade or purer and were obtained from Sigma-Aldrich.

According to the Hildebrand theory, affine solvents are those having a Hildebrand parameter, δ, similar to that of natural rubber.[33] We have defined nonaffine solvents as those that have $\Delta\delta$ ($|\delta_{NR} - \delta_{solvent}|$) of at least 3.4 MPa$^{0.5}$.

The values of strain fixity and strain recovery were obtained by using the following equations:

$$R_f = \frac{\varepsilon_f}{\varepsilon_{m,80}}$$

$$R_r = \frac{\varepsilon_{m,80} - \varepsilon_p}{\varepsilon_{m,80}}$$

where ε_f is fixed strain, and $\varepsilon_{m,80}$ is 80% of maximum strain. The dimension changes were measured with a conventional ruler using markings on the samples. R_r values were determined for all samples to at least 99%.

Determination of Trigger Temperature. Trigger temperatures were obtained by using a thermal mechanical analyzer TMA 2940 (TA Instruments, Inc.). The penetration probe was used with a preload force of 0.05 N to measure the thickness increase upon continuously increasing the temperature with 1 K min^{-1}. To evaluate the trigger process kinetic, we differentiated the relative thickness change ε_t with respect to temperature.[25] The trigger temperature T_{Trig} is at the maximum of the curve.

ASSOCIATED CONTENT

Supporting Information

Mooney-Rivlin- and TMA plots of differently stored and programmed SMNR samples. This material is available free of charge via the Internet at http://pubs.acs.org.

AUTHOR INFORMATION

Corresponding Author

*E-mail: joerg.tiller@udo.edu.

Author Contributions

The manuscript was written through contributions of all authors. All authors have given approval to the final version of the manuscript.

Notes

The authors declare no competing financial interest.

ACKNOWLEDGMENTS

The authors thank Continental Reifen Deutschland GmbH, in particular, Dr. Fred Waldner, for providing nonvulcanized natural rubber.

DOI: 10.1021/am507184c
ACS Appl. Mater. Interfaces 2015, 7, 1486–1490

REFERENCES

(1) Lendlein, A.; Kelch, S. Shape-Memory Polymers. *Angew. Chem., Int. Ed. Engl.* **2002**, *41*, 2034−2057.
(2) Quitmann, D.; Gushterov, N.; Sadowski, G.; Katzenberg, F.; Tiller, J. C. Solvent-Sensitive Reversible Stress-Response of Shape Memory Natural Rubber. *ACS Appl. Mater. Interfaces* **2013**, *5*, 3504−3507.
(3) Quitmann, D.; Gushterov, N.; Sadowski, G.; Katzenberg, F.; Tiller, J. C. Environmental Memory of Polymer Networks under Stress. *Adv. Mater.* **2014**, *26*, 3441−3444.
(4) Zhu, Y.; Hu, J.; Luo, H.; Young, R. J.; Deng, L.; Zhang, S.; Fan, Y.; Ye, G. Rapidly Switchable Water-Sensitive Shape-Memory Cellulose/Elastomer Nano-Composites. *Soft Matter* **2012**, *8*, 2509−2517.
(5) Wang, C. C.; Zhao, Y.; Purnawali, H.; Huang, W. M.; Sun, L. Chemically Induced Morphing in Polyurethane Shape Memory Polymer Micro Fiber/Springs. *React. Funct. Polym.* **2012**, *72*, 757−764.
(6) Lu, H.; Huang, W. M. A Phenomenological Model for the Chemo-Responsive Shape Memory Effect in Amorphous Polymers Undergoing Viscoelastic Transition. *Smart Mater. Struct.* **2013**, *22*, 115019.
(7) Huang, W. M.; Zhao, Y.; Wang, C. C.; Ding, Z.; Purnawali, H.; Tang, C.; Zhang, J. L. Thermo/Chemo-Responsive Shape Memory Effect in Polymers: A Sketch of Working Mechanisms, Fundamentals and Optimization. *J. Polym. Res.* **2012**, *19*, 1−34.
(8) Heuwers, B.; Quitmann, D.; Katzenberg, F.; Tiller, J. C. Stress-Induced Melting of Crystals in Natural Rubber: A New Way to Tailor the Transition Temperature of Shape Memory Polymers. *Macromol. Rapid Commun.* **2012**, *33*, 1517−1522.
(9) Heuwers, B.; Quitmann, D.; Hoeher, R.; Reinders, F. M.; Tiemeyer, S.; Sternemann, C.; Tolan, M.; Katzenberg, F.; Tiller, J. C. Stress-Induced Stabilization of Crystals in Shape Memory Natural Rubber. *Macromol. Rapid Commun.* **2013**, *34*, 180−184.
(10) Lendlein, A.; Jiang, H.; Jünger, O.; Langer, R. Light-Induced Shape-Memory Polymers. *Nature* **2005**, *434*, 879−882.
(11) Mohr, R.; Kratz, K.; Weigel, T.; Moneke, M.; Lendlein, A. Initiation of Shape-Memory Effect by Inductive Heating of Magnetic Nanoparticles in Thermoplastic Polymers. *Proc. Natl. Acad. Sci. U.S.A.* **2006**, *103*, 3540−3545.
(12) Heuwers, B.; Beckel, A.; Krieger, A.; Katzenberg, F.; Tiller, J. C. Shape Memory Natural Rubber: An Exceptional Material for Strain and Energy Storage. *Macromol. Chem. Phys.* **2013**, *214*, 912−923.
(13) Hoeher, R.; Raidt, T.; Krumm, C.; Meuris, M.; Katzenberg, F.; Tiller, J. C. Tunable Multiple-Shape Memory Polyethylene Blends. *Macromol. Chem. Phys.* **2013**, *214*, 2725−2732.
(14) Hoeher, R.; Raidt, T.; Rose, M.; Katzenberg, F.; Tiller, J. C. Recoverable Strain Storage Capacity of Shape Memory Polyethylene. *J. Polym. Sci., Part B: Polym. Phys.* **2013**, *51*, 1033−1040.
(15) Ahn, S.; Deshmukh, P.; Kasi, R. M. Shape Memory Behavior of Side-Chain Liquid Crystalline Polymer Networks Triggered by Dual Transition Temperatures. *Macromolecules* **2010**, *43*, 7330−7340.
(16) Lee, K. M.; Bunning, T. J.; White, T. J. Autonomous, Hands-Free Shape Memory in Glassy, Liquid Crystalline Polymer Networks. *Adv. Mater.* **2012**, *24*, 2839−2843.
(17) Brinson, L. C. One-Dimensional Constitutive Behavior of Shape Memory Alloys: Thermomechanical Derivation with Non-Constant Material Functions and Redefined Martensite Internal Variable. *J. Intell. Mater. Syst. Struct.* **1993**, *4*, 229−242.
(18) Lendlein, A.; Langer, R. Biodegradable, Elastic Shape-Memory Polymers for Potential Biomedical Applications. *Science* **2002**, *296*, 1673−1676.
(19) Van Humbeeck, J. Non-Medical Applications of Shape Memory Alloys. *J. Mater. Sci. Eng. A* **1999**, *273*−*275*, 134−148.
(20) Katzenberg, F.; Heuwers, B.; Tiller, J. C. Superheated Rubber for Cold Storage. *Adv. Mater.* **2011**, *23*, 1909−1911.
(21) Cui, J.; Kratz, K.; Lendlein, A. Adjusting Shape-Memory Properties of Amorphous Polyether Urethanes and Radio-Opaque Composites thereof by Variation of Physical Parameters during Programming. *Smart Mater. Struct.* **2010**, *19*, 065019.
(22) Behl, M.; Lendlein, A. Triple-Shape Polymers. *J. Mater. Chem.* **2010**, *20*, 3335−3345.
(23) Xie, T. Tunable Polymer Multi-Shape Memory Effect. *Nature* **2010**, *464*, 267−270.
(24) Xie, T. Recent Advances in Polymer Shape Memory. *Polymer.* **2011**, *52*, 4985−5000.
(25) Quitmann, D.; Dibolik, M.; Katzenberg, F.; Tiller, J. C. Altering the Trigger-Behavior of Programmed Shape Memory Natural Rubber (SMNR) by Solvent Vapor. *Macromol. Mater. Eng.* **2015**, *300* (1), 25−30.
(26) Marand, H.; Huang, Z. Isothermal Lamellar Thickening in Linear Polyethylene: Correlation between the Evolution of the Degree of Crystallinity and the Melting Temperature. *Macromolecules* **2004**, *37*, 6492−6497.
(27) Wunderlich, B.; Melillo, L. Morphology and Growth of Extended Chain Crystals of Polyethylene. *Makromol. Chem.* **1968**, *118*, 250−264.
(28) Saalwaechter, K.; Chassé, W.; Sommer, J.-U. Structure and Swelling of Polymer Networks: Insights from NMR. *Soft Matter* **2013**, *9*, 6587−6593.
(29) Schloegl, S.; Trutschel, M.-L.; Chasse, W.; Riess, G.; Saalwaechter, K. Entanglement Effects in Elastomers: Macroscopic vs Microscopic Properties. *Macromolecules* **2014**, *47*, 2759−2773.
(30) Ronan, S.; Alshuth, T.; Jerrams, S.; Murphy, N. Long-Term Stress Relaxation Prediction for Elastomers Using the Time-Temperature Superposition Method. *Mater. Des.* **2007**, *28*, 1513−1523.
(31) Tobolsky, A. V.; Prettyman, I. B.; Dillon, J. H. Stress Relaxation of Natural and Synthetic Rubber Stocks. *J. Appl. Phys.* **1944**, *15*, 380−395.
(32) Mooney, M. A Theory of Large Elastic Deformation. *J. Appl. Phys.* **1940**, *11*, 582−592.
(33) Hildebrand, J. Thermodynamic Aspects of the Theory of Non-Electrolytic Solutions. *Chem. Rev.* **1936**, *18*, 315−323.

DOI: 10.1021/am507184c
ACS Appl. Mater. Interfaces 2015, 7, 1486−1490